

The Associative Properties of Some Amphiphilic Fullerene Derivatives

Guido Angelini,^[a] Claudia Cusan,^[b] Paolo De Maria,^{*[a]} Antonella Fontana,^[a] Michele Maggini,^[d] Marco Pierini,^{*[c]} Maurizio Prato,^[b] Stefano Schergna,^[d] and Claudio Villani^[c]

Keywords: Aggregation / Amphiphiles / Fullerenes / Partition coefficient

The hydrophilic vs. hydrophobic balance for five C₆₀ derivatives (**FD1–5**) bearing one hydrophilic addend has been evaluated by means of useful descriptors derived from (i) aggregation measurements in aqueous/organic mixtures, (ii) partition measurements between *n*-octanol and water (log *P*_{m/a}), and (iii) retention factors in reverse-phase

chromatography (log *k*_w). Aggregates of **FD1–5** have been obtained both in water and in aqueous organic mixtures. The dimension of the aggregates has been estimated by gel-permeation chromatography.

(© Wiley-VCH Verlag GmbH & Co. KGaA, 69451 Weinheim, Germany, 2005)

Introduction

There is clear evidence from a number of recent studies that the special geometric and electronic properties of fullerenes^[1] could find new applications in different fields such as materials technology,^[2,3] biology^[4] and medicinal chemistry.^[5–7]

However, the fact that these molecules are highly hydrophobic hampers their direct solubilization in water and, more generally, in polar solvents. Functionalization with hydrophilic addends represents a direct strategy for making fullerenes relatively soluble in water. It has been found that these derivatives can dissolve either in the form of monomers or as supramolecular aggregates.^[8]

In particular, water-soluble C₆₀ multiple adducts prefer to dissolve as monomers in water and aqueous organic solvents,^[9–11] whereas monoadducts display a strong tendency to form clusters,^[10,12–18] depending upon the particular hydrophilic/hydrophobic balance in their molecular structures and the polarity^[7] of the medium. The present work intends to identify reliable descriptors of the hydrophilic/hydro-

phobic ratio for C₆₀ derivatives functionalized with hydrophilic addends.

Aggregation measurements in aqueous/organic mixtures, partition measurements between *n*-octanol and water and retention factors in reverse-phase chromatography refer to definite properties of the studied substances and provide useful reference parameters for predicting the solubility and aggregation behaviour of amphiphilic fullerene derivatives. Moreover, an in-depth investigation of the interactions that drive both the autoassociation process of the **FD1–5** (Scheme 1) in solution and the chromatographic retention of **FD1–4** on an apolar stationary phase is presented. The free-energy changes associated with the aggregation of **FD1–5** and their transfer from the aggregate form in water to the monomer form in *n*-octanol are also estimated.

Results and Discussion

Cluster formation from amphiphilic fullerene derivatives was promoted by prolonged sonication and/or by the addition of small quantities of an appropriate organic modifier.^[11,13,14,17–19]

A general protocol has been proposed recently^[12] in which a standardized procedure for obtaining fully aqueous solutions of AFE aggregates (Scheme 2) is described.

The dimensions^[12] of the clusters of AFE were those expected for typical colloidal particles (diameter about 120 nm) characterized by fractal^[20] structures.

A preliminary analysis shows that compounds **FD1–5** are relatively soluble in organic solvents of moderate polarity (e.g. THF, CHCl₃, CH₂Cl₂, *n*C₈H₁₇OH) and sparingly soluble in apolar or polar solvents (e.g. *n*C₆H₁₄, CH₃CN, CH₃OH). The same five derivatives are virtually insoluble in water. However, aqueous solutions of aggregates of **FD1–**

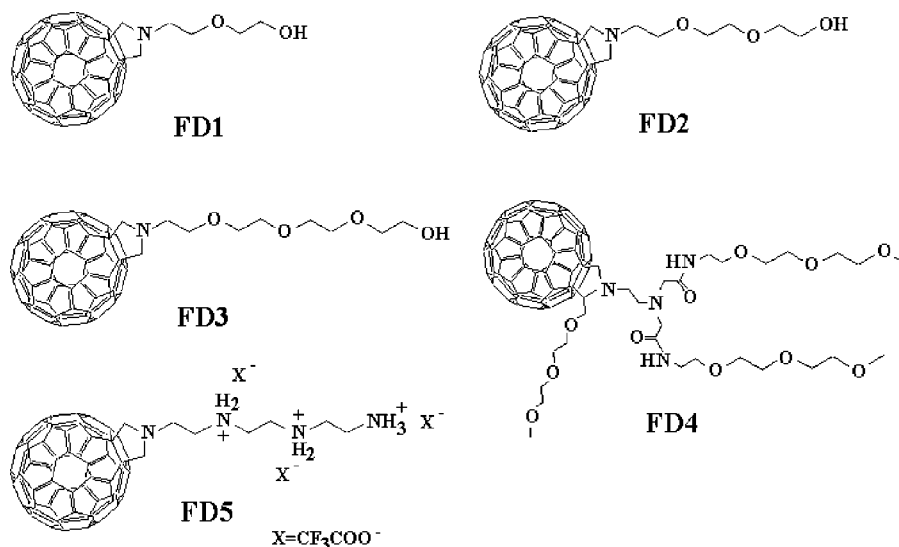
[a] Dipartimento di Scienze del Farmaco, Università “G. d’Annunzio”, Via dei Vestini 31, 66013 Chieti, Italy
Fax: +39-0871-355-5204
E-mail demaria@unich.it

[b] Dipartimento di Scienze Farmaceutiche, Università di Trieste, Piazzale Europa 1, 34127 Trieste, Italy

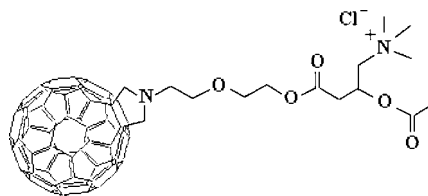
[c] Dipartimento di Studi di Chimica e Tecnologia delle Sostanze Biologicamente Attive, Università “La Sapienza”, Piazzale A. Moro 5, 00185 Roma, Italy
Fax: +39-06-4991-2780
E-mail marco.pierini@uniroma1.it

[d] Dipartimento di Scienze Chimiche and ITM-CNR, Università di Padova, Via Marzolo 1, 35131 Padova, Italy

Supporting information for this article is available on the WWW under <http://www.eurjoc.com> or from the author.



Scheme 1.



Scheme 2. Structure of AFE.

5 up to a concentration of 2×10^{-5} M can be prepared from a stock THF solution by successive additions of water, followed by evaporation of THF till the complete removal of the organic solvent, according to a previously described protocol.^[12]

Colloidal solutions of **FD4** and **FD5** can also be obtained by sonication of a solid sample in water. However, this method did not give reproducible results and only low concentrations of aggregates could be obtained ($< 5 \times 10^{-6}$ M). The presence of aggregates in solution is demonstrated by the analysis of the corresponding UV/Vis spectra (see, for example, Figure 1). Clear differences emerge from the comparison of the spectra obtained in solution of apolar solvents or in solvents of moderate polarity (e.g. $n\text{C}_6\text{H}_{14}$, THF, CHCl_3 , $n\text{C}_8\text{H}_{17}\text{OH}$), where **FD1–5** are present in monomeric form, with the spectra obtained in aqueous solutions. In fact, the spectra of the monomers display sharp absorptions at 254 and 430 nm and a shoulder at 320 nm, with very similar ϵ values for the five investigated derivatives (see, for example, Figure 1, solid line). On the other hand, the spectra of the aggregates of the five FDs in water (or in aqueous THF solutions with percentage (v/v) of THF < 20 for **FD1–4** and < 10 for **FD5**) are characterized by a wide broadening of the absorption band near 254 nm and by the fact that the ϵ values decrease at lower and increase at higher wavelengths. In addition, the weak peak at 430 nm disappears for the aqueous aggregates (see Figure 1, broken

and dashed lines). The formation of aggregates in aqueous THF solutions was followed starting from a pure THF solution of the fullerene derivative by progressively increasing the amounts of water.

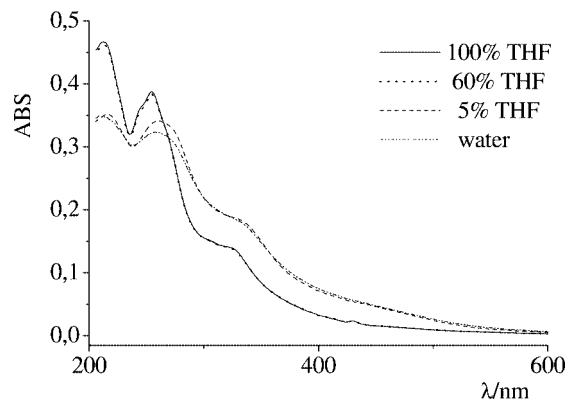


Figure 1. UV/Vis spectra of **FD3** in 100% THF (—), in aqueous THF solutions [60% (v/v) THF (·····), 5% (v/v) THF (----)] and in water (-·-·-·-); [**FD3**] = 5×10^{-5} M.

Typical sigmoidal aggregation curves are obtained for **FD1–5** by plotting $\Delta\text{ABS}_{(254-430)\text{norm}}$ ^[21] against the Hildebrand polarity index,^[22] δ_{H} , of the solvent mixtures in aqueous THF solutions (see Figure 2<yigr2>) and in aqueous CH_3OH solutions. The aggregation process can be described by Equation (1).

$$\Delta\text{ABS}_{(254-430)\text{norm}} = 100/[1 + 10^{(\delta_{\text{H}} - \text{API})/a}] \quad (1)$$

The variable a is an adjustable parameter (which refers to the gradient of variation of ΔABS as a function of δ_{H}) and API is an Aggregation Polarity Index characteristic of each FD derivative. The values of API obtained from a regression analysis of Equation (1) are reported in Table 1.

Table 1. API values, $\log P_{m/a}$, ΔG_{tr} and $\log k_w$ for DF derivatives.

	(H ₂ O/THF) API [kcal dm ⁻³] ^{1/2}	a	(H ₂ O/CH ₃ OH) API [kcal dm ⁻³] ^{1/2}	a	$\log P_{calc}$	$\log P_{m/a}$	ΔG_{tr} [kcal mol ⁻¹]	$\log k_w^{C18}$
FD1	17.67 ± 0.19	0.020 ± 0.002			-0.9	-0.88	1.21	4.26
FD2	18.03 ± 0.01	0.23 ± 0.02			-1.07	-1.10	1.50	3.96
FD3	18.56 ± 0.02	0.22 ± 0.04			-1.23	-1.15	1.58	3.86
FD4	19.96 ± 0.04	0.85 ± 0.05	18.13 ± 0.06	0.71 ± 0.16	1.01	-0.05	0.06	3.51
FD5	20.94 ± 0.07	1.17 ± 0.14			8.65	1.11	-1.52	

For a given FD derivative, API represents the solvent polarity corresponding to a 50% variation of ΔABS .

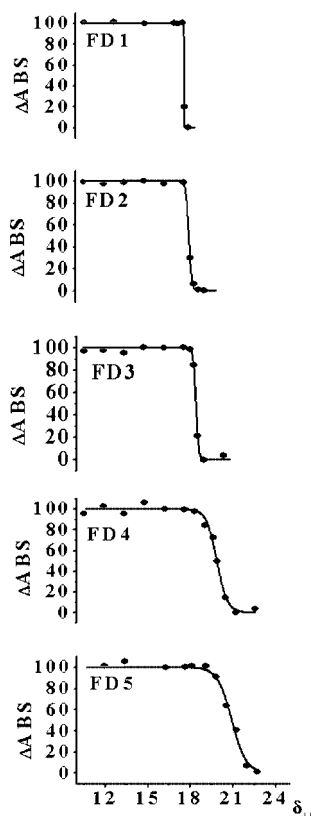


Figure 2. Aggregation of DFs in aqueous THF solutions: plots of $\Delta ABS_{(254-430)norm}^{[21]}$ against δ_H .

It appears that the API values depend both on the hydrophilic/hydrophobic ratio within the molecular structure of the particular FD and, to a lesser extent, on the organic co-solvent used (THF or CH₃OH). Indeed, the aggregation curve of **FD4** obtained in aqueous CH₃OH solutions gives an API of 18.1 (kcal dm⁻³)^{1/2} which is some 1.9 units lower than the value of 20.0 obtained in aqueous THF solutions. In order to use API as a physical constant of each FD derivative, it is necessary to refer to a given FD concentration. This is because, at a given solvent composition, the degree of aggregation of the substrate increases with concentration. Measurements of APIs for **FD2** and **FD3** at different concentrations clearly show that the aggregation of these substrates is anticipated (i.e. occurs at lower δ_H values)

when the concentration of the FD is increased. In other words, the whole curve (of the type shown in Figure 2) is shifted towards regions of lower polarity of the solvent mixture at higher FD concentration. The value of API, of course, decreases accordingly. The experimental API² values are linearly related to the logarithm of the molar concentrations of **FD2** and **FD3** as shown in Equation (2) and (3), respectively.

$$API^2_{FD2} = -49.4 \log [FD2] + 66.6; n = 4; r^2 = 0.98 \quad (2)$$

$$API^2_{FD3} = -38.3 \log [FD3] + 138.1; n = 7; r^2 = 0.96 \quad (3)$$

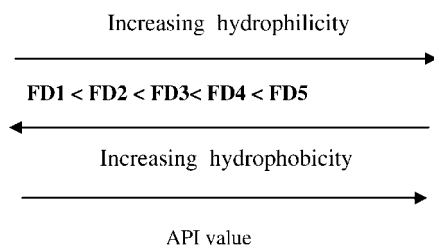
The intercepts are the notional API² values of 1 M solutions of the two substrates.

The above results suggest that the value of API at a given concentration (5×10^{-6} mol dm⁻³ in Table 1) is a reliable descriptor of the tendency of the FD to form molecular aggregates in a particular solvent mixture.

It should be recalled, in this context, that the polarity index, δ_H , depends on the vaporization enthalpy, ΔH_{vap} , and the molar volume, V , of the solvent according to Equation (4).^[22]

$$\delta^2_H = (\Delta H_{vap} - RT)/V \quad (4)$$

Thus, δ_H is directly related to the energy of cohesion of the molecules of the solvent. From an energy point of view, higher API values point to a higher energy request for the formation of cavities within the solvent where the aggregate units can be hosted. By the same token, higher API values suggest weaker solvophobic interactions among the FD molecules in a given solvent, for example pure water. In other words, to promote the aggregation of a relatively hydrophilic FD, it is necessary to increase the solvophobic intermolecular interaction with a higher percentage of the more-polar component of the solvent mixture. From the API values collected in Table 1 the studied FDs can be ranked according to the following order of increasing hydrophilic character.



It is known that solvophobic interactions acting between lipophilic species being transferred from less-polar or apolar solvents, (1), into more polar solvents, (2), are mainly entropic in origin,^[23,24] and often it is these solvophobic interactions that dominate the free-energy change of cavitation. The entropy contribution prevails over the enthalpy contribution in the transfer process when the polarity difference between the two solvents (1) and (2) is small (e.g. negligible differences in the VdW interactions between the solute and the two solvents).^[25,26] The free-energy change for the creation of a cavity in a solvent, ΔG_{cav} , is taken as the work necessary to expand the liquid surface by a quantity equal to the solute molecular surface, A , against the surface tension, γ , of the solvent. Thus, ΔG_{cav} can be calculated^[27] by Equation (5). The factor κ corrects γ for the curvature of the cavity.^[28,29]

$$\Delta G_{\text{cav}} = \kappa \gamma A \quad (5)$$

In the autoassociation processes investigated, the aggregation always starts and terminates within a narrow range of polarity of the medium. Under these conditions, it is reasonable to take the cavitation free-energy change, $\Delta \Delta G_{\text{cav}}$, as a measure of the solvophobic interactions taking place during autoassociation.

The values of $\Delta \Delta G_{\text{cav}}$ can be estimated from the aggregation curves (Figure 2) of **FD1–5** as follows. In the absence of aggregation $\Delta \Delta G_{\text{cav}}$, when the polarity of the solvent passes from δ_{H1} to δ_{H2} , is given by Equation (6).

$$\Delta \Delta G_{\text{cav}} = (\kappa_2 \gamma_2 - \kappa_1 \gamma_1) A \quad (6)$$

The values of δ_{H1} and δ_{H2} , at which the aggregation starts and terminates, can be extracted graphically from the aggregation plots (Figures 2 and 3). The corresponding surface tensions γ_1 and γ_2 can be interpolated from a plot of experimental γ values against solvent composition. The quantity A can be calculated by molecular mechanics.

The percentage of reduction, upon association, of the solute surface area exposed to the solvent, $\% \Delta A$, required to minimize the free energy of the system, can be calculated from Equation (7).

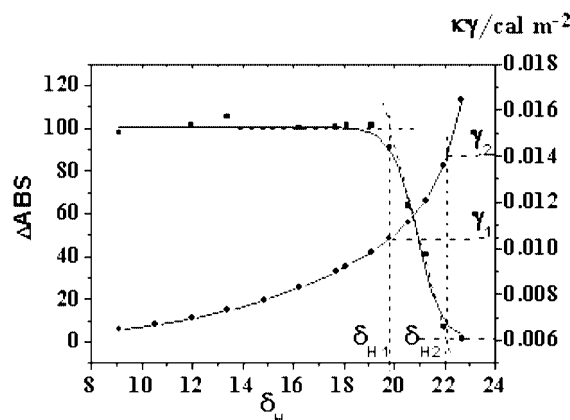


Figure 3. Plots of $\Delta \text{ABS}_{(254-430)\text{norm}}$ for **FD5** (full squares) and of corrected γ [see Equation (5)] (full circles) against Hildebrand's δ_{H} values of aqueous THF mixtures.

$$\% \Delta A = |(\kappa_1 \gamma_1 / \kappa_2 \gamma_2 - 1)| \times 100 \quad (7)$$

The values of $\% \Delta A$ and $\Delta \Delta G_{\text{cav}}$ for **FD1–5** are collected in Table 2. Measurements carried out with six different substrate concentrations for **FD2** and **FD3**, in the range 8×10^{-5} to 5×10^{-6} M, show that $\Delta \Delta G_{\text{cav}}$ is independent of concentration (Table 2, last column). As expected from the API values, these results point to a rapid increase in the solvophobic interactions between the molecules of solute when the hydrophilicity of FDs and the polarity of the solvent increase. At the same time a reduction of the molecular surface of the fullerene derivative exposed to the solvent is observed. However, the different values of $\% \Delta A$, calculated from Equation (7), suggest that **FD1–5** form supramolecular aggregates of different size and/or morphology, with larger and more densely packed aggregates in solvents of higher polarity. To support this point, transmission electron microscopy pictures were taken of samples prepared using different percentages of organic solvents. Although the samples in the TEM investigations were prepared by allowing the solvent to evaporate, the dissimilarities of the transmission electron microscopy pictures obtained could give additional information on the aggregation process. Figure 4 shows representative TEM pictures of aggregates generated from solutions of 5×10^{-5} M **FD3** as a function of the (v/v) composition of the aqueous THF solution. Aggregated monodisperse clusters were observed in water and in aqueous THF solution with 5% (v/v) THF. The sizes of the individual cluster are 30–50 nm (see a and b in Figure 4) and a fractal structure characterizes the cluster aggregates. **FD3** does not show well-shaped aggregates from mixtures with $\delta_{\text{H}} < \text{API}$ (API = 17.4 at [**FD3**] = 5×10^{-5} M [see c in Figure 4 from aqueous THF solution with 60% (v/v) THF]). Under these conditions individual clusters cannot be identified within the few observable aggregates and the image is characterized by a high background noise.

Table 2. Solute molecular surface (A) calculated by molecular mechanics, cavitation free-energy change ($\Delta\Delta G_{\text{cav}}$) and percentage of reduction upon association of the solute surface area exposed to the solvent ($\% \Delta A$) for FD derivatives calculated at constant FD concentrations.

A [Å ²]	mix(H ₂ O/THF) [FD] = 5×10^{-6} M		mix(H ₂ O/THF) 8×10^{-5} > [FD] > 5×10^{-6} M	
	$\Delta\Delta G_{\text{cav}}$ [kcal mol ⁻¹]	$\% \Delta A$	$\Delta\Delta G_{\text{cav}}$ [kcal mol ⁻¹]	
FD1 744	0.27	0.66	–	
FD2 834	1.39	2.98	1.33 ± 0.16	
FD3 919	1.69	3.18	1.95 ± 0.45	
FD4 1396	12.55	13.11	–	
FD5 1132	21.42	23.02	–	

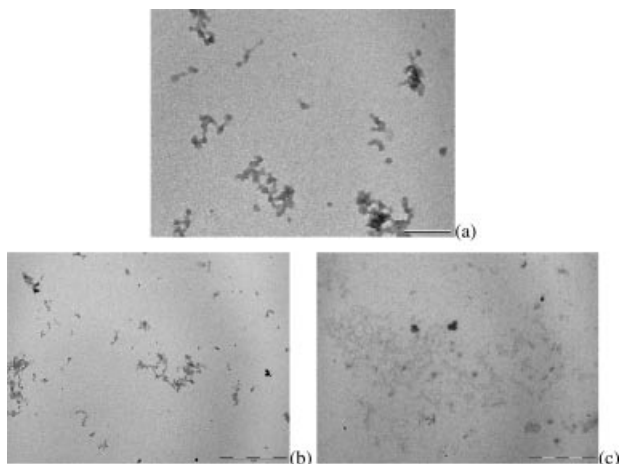


Figure 4. Representative TEM pictures of aggregates of **FD3** in water (a), in aqueous THF solution with 5% (v/v) THF (b) and 60% (v/v) THF (c). The UV/Vis spectra corresponding to the solutions of pictures (a), (b) and (c) are reported in Figure 1 as the broken, dashed and solid lines, respectively. The initial **FD3** concentration is 5×10^{-5} M in all cases. Scale bars are 200 nm, 500 nm and 1 μm in (a), (b) and (c), respectively.

Solutions of **FD2** and **FD3** in THF and in water were also analyzed in reverse-phase HPLC experiments (RP-HPLC) using a macroporous C4 column (pore diameter = 300 Å) and a diode-array detector. Aqueous THF mixtures of appropriate composition (near those required for the aggregation of the two derivatives) were used as eluents. After elution, either the THF solution (where **FD2** and **FD3** are present in the form of monomers) or the aqueous solution (where they are present in the form of aggregates) display two distinct peaks in their chromatograms which can be attributed to the aggregate (shorter elution time) and the monomer (longer retention time) from the known UV/Vis spectra of the two species (Figure 5).

However, the proportion of the monomers is much higher than that of the aggregates in THF solution, and vice versa in aqueous solution. Apparently, aggregation occurs in the column in the former case, while disaggregation occurs in the column in the latter case. It should also be outlined that the aggregates elute before the dead volume in both cases. This points to their exclusion from the pores of the stationary phase and suggests a diameter greater than

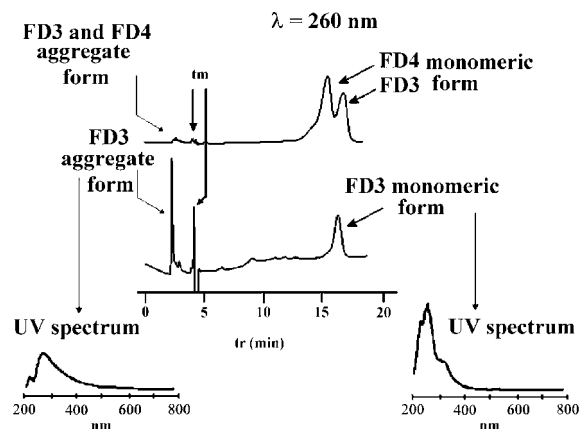


Figure 5. Chromatograms displaying both the monomer and the aggregate forms of **FD3** and **FD4**.

30 nm for the aggregated FDs. HPLC results suggest that the UV/Vis spectral changes observed in the aggregation curves of Figure 2 depend on an increasing fraction of monomeric FD, which is progressively transformed into the corresponding supramolecular aggregate (cluster), rather than on a steady increase of the dimensions of the aggregate upon addition of water to the solvent mixture.

Static light-scattering experiments, carried out on aqueous AFE^[12] solutions (Scheme 2) afforded, for AFE aggregates, an average diameter of 120 nm. Gel-permeation HPLC experiments with aqueous solutions of **FD2**, **FD3** and AFE, as a reference compound, indicated an average aggregate diameter greater than 120 nm. The dimensions of the aggregated clusters of aqueous **FD3**, pictured by TEM (see Figure 4a), span from 80 to 300 nm. Neglecting the largest aggregates, which presumably form during specimen preparation, the medium-sized clusters (with a mean diameter of about 140 nm) give a realistic idea of a typical supramolecular fractal aggregate in solution and are in agreement with the GP-HPLC results.

Further insight into the hydrophilic/hydrophobic ratios of **FD1–5** was obtained by measuring the *n*-octanol/water partition coefficient by the shake-flask technique. The monomer/aggregate partition coefficients, $P_{m/a}$, were calculated by measuring spectrophotometrically their respective concentration in both phases (from calibration curves obtained in water and in *n*-octanol), after 24 h stirring and when a conventional equilibrium had been established in all cases. Inspection of the results collected in Table 1 shows that the values of $\log P_{m/a}$ are low and quite similar for **FD1–3**. The length of the oxyethylene chain linked to the pyrrolidine nitrogen of **FD1–3** scarcely affects the hydrophilic surface of the corresponding aqueous aggregates, thus leaving the fraction of the aggregates transferred from the aqueous to the organic phase essentially unchanged.

The $\log P_{m/a}$ values measured for **FD4** and **FD5** (which have higher API values and hence higher hydrophilic character than **FD1–3**) are considerably higher than the $\log P_{m/a}$ values of **FD1–3**. It might appear surprising that the more hydrophilic aggregates are transferred into the organic phase at higher proportions. However, this behaviour can

be understood by taking into account the following effects: (i) the reduced intensity of the hydrophobic forces among the solute molecules makes the cluster relatively unstable in aqueous solutions; (ii) the individual FD molecules are inefficiently hydrated due to the presence of the large C_{60} sphere (the FD monomers are nearly insoluble in aqueous solutions); (iii) the same FD molecules are efficiently solvated by *n*-octanol (the FDs are relatively soluble in this solvent). The entropy change associated with the transfer of the aggregate from water to its monomeric form in *n*-octanol should be highly positive for all the studied derivatives. Assuming that the entropy value of the monomers in *n*-octanol is approximately the same for all the FDs, the ΔS_{tr} should be essentially determined by the entropy value of the aggregate in aqueous solution. The clusters of the more hydrophilic FDs and their hydration shells should be considerably more ordered (lower entropy) than those of the less-hydrophilic FDs making the entropy contribution to ΔG_{tr} for the former derivatives more favourable. It is interesting that the $\log P_{calc}$ values referred to the FDs hypothetically present in their monomeric forms in both phases, calculated with a commercially available software program (Table 1), are linearly correlated to the experimental $P_{m/a}$ values according to Equation (8).

$$\log P_{calc} = 4.22 \log P_{m/a} + 3.04 \quad (n = 5 \quad r^2 = 0.931) \quad (8)$$

The free-energy changes, ΔG_{tr} , of transfer of the FDs from the aggregate form in water to the monomeric form in *n*-octanol can be calculated from Equation (9).

$$\Delta G_{tr} = -RT \ln P_{m/a} \quad (9)$$

The results are collected in Table 1. The measured API and $\log P_{m/a}$ values allow us to relate the autoassociation properties of **FD1–5**, in water or in aqueous organic mixtures, to the hydrophilic/hydrophobic ratio within their molecular structures. This ratio, though, can be more directly studied by reverse-phase HPLC experiments as follows.

It is well known that chromatographic retention data collected on non-polar stationary phases can be used to extract quantitative information on solute hydrophobicity. Several studies have shown the existence of a correlation between logarithmic retention factors in reverse-phase chromatography and logarithmic *n*-octanol/water partition coefficients for a given set of solutes.^[30] Retention in reverse-phase chromatography increases with solute lipophilic character and, for a given combination of solute and stationary phase, with the water content of the mobile phase. When binary organic solvent–water mixtures are used as the eluent, logarithmic retention decreases linearly with concentration of the organic solvent [Equation (10)].

$$\log k = \log k_w - S\varphi \quad (10)$$

Variable k is the observed retention factor, k_w is a measure of solute retention with pure water as the eluent, S is a constant for a given solute and φ is the volume fraction of the organic solvent in the eluent.

Retention of solutes **FD1–4** was monitored on an octadecylsilylated stationary phase using aqueous THF mixtures

where the organic modifier content (volume fraction, φ) varied by 0.05 increments from 0.45 to 0.85. **FD5** was excluded from the HPLC investigations as its elution was impossible with aqueous THF eluents. For each eluent composition a decreasing retention factor in the order **FD1** > **FD2** > **FD3** > **FD4** for the four solutes was observed (Figure 6). This order is consistent with the decreasing lipophilicity of the four FDs.

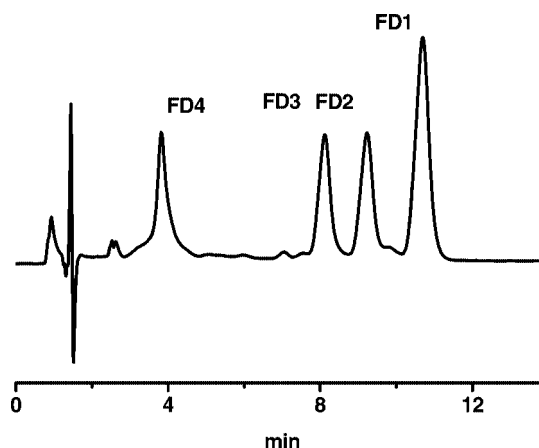


Figure 6. Chromatogram of **FD1–4** obtained from an octadecylsilylated stationary phase using aqueous THF mixture as the eluent.

Plots of logarithmic retention vs. eluent composition gave straight lines in all cases, and extrapolation of these lines to $\varphi = 0$ gave the $\log k_w$ values for **FD1–4** listed in Table 1. However, the $\log k_w$ values do not change much on passing from **FD1** to **FD4**. Clearly, the stepwise addition of ethoxy units to the fulleropyrrolidine core has only a marginal (negative) effect on the solute lipophilicity. Should the linear elongation of the polyethoxy chain have a mere subtractive effect on lipophilicity, one could predict by extrapolation a $\log k_w$ equal to zero (equal affinity of the solute for the two phases) when the number of ethoxy units is about 20. The reduced lipophilicity of **FD4**, where the ethoxy units are distributed over three different chains, is due to the large number of polar fragments and, to some extent, to the overall branching of the C_{60} addend.

In order to establish the exact relationship between $\log k_w$ and $\log P$ data, we carried out the same chromatographic analysis on four polycyclic aromatic hydrocarbons (PAHs; anthracene, triphenylene, benzo[*a*]pyrene and coronene) whose $\log P$ values are known.^[31] Chromatographic data show that $\log k_w$ values for these PAHs are linearly related to their $\log P$ according to Equation (11).

$$\log P = 4.19(\log k_w) - 8.46 \quad (r^2 = 0.98; n = 4) \quad (11)$$

The logarithmic *n*-octanol/water coefficients for the fullerene derivatives calculated using Equation (11) are 9.39, 8.13, 7.71 and 6.25 for **FD1**, **FD2**, **FD3** and **FD4**, respectively.

These figures can be compared with the estimated value of $\log P = 12.6$ for pristine C_{60} . It is seen that the introduction of the polar fragments has a sizeable effect on the hydrophilic/hydrophobic ratio, which is of course shifted

towards the hydrophilic side. However, the water solubilities of the studied fullerene derivatives are still very low and comparable to those of medium-sized PAHs.

In addition, a linear correlation between $\log k_w$ and API² values was observed. This linearity is linked to the intrinsic similarity of the two processes we are observing: interaction of the fullerene derivatives with the apolar stationary phase ($\log k_w$) and autoassociation to form the aggregates (API²). Clearly both processes are dominated by solvophobic interactions.

As previously stated, $\log k_w$ and $\log P$ for several systems are linearly related. With the present work we show that a similar correlation also exists [Equation (12)] between $\log k_w$ and $\log P_{m/a}$ for the homologous series **FD1–3**.

$$\log k_w = 1.47 \log P_{m/a} + 5.56 \quad (n = 3, r^2 = 0.9987) \quad (12)$$

On the other hand, the strong deviation of **FD4** from the correlation of Equation (12) suggests that the hydrophilic appendix of **FD4** is involved in specific solute–solvent interactions, upon transfer between *n*-octanol and water, which have no parallel counterparts in the chromatographic process. These interactions are probably due to the hydrogen-bonding properties of *n*-octanol as compared to the hydrocarbon-like properties of the apolar stationary phase.

Conclusions

The different approaches adopted in this paper clearly show that useful descriptors can be obtained for the hydrophilic/hydrophobic balance for the investigated FDs. Aggregation measurements in aqueous/organic mixtures, partition measurements between *n*-octanol and water and retention factors in reverse-phase chromatography are particularly convenient for describing the reversible transition from the monomeric to the aggregated forms of the FDs when passing progressively from organic solvents to aqueous solutions. Some interesting linear relationships have been found between the investigated parameters, which refer directly to the aggregation equilibria. Differences in morphologies and in size of the aggregates have been visualized in the absence of solvent by TEM measurements. The importance of solvophobic interactions in the aggregation process has been highlighted.

Experimental Section

Liquid Chromatography: HPLC analyses were performed with a TSP chromatograph equipped with a P2000 pump, a UV6000 LP diode array detector and a Reodyne 7125 injector. In RP-HPLC experiments a Hypersil HyPURITY® C4 5 μ m 250 \times 4.0 mm ID column or a Hypersil BDS C18 3 μ m 100 \times 4.6 mm ID column were used. In GP-HPLC experiments TSK GEL PW 6000 column was used and the fractionation range was tested towards blue dextrane (Sigma) and a dilute solution of FeSCN to evaluate the exclusion and the maximum inclusion volume of the resin, respectively.

Partition Experiments: Partition experiments between *n*-octanol and water were carried out at 25.0 \pm 0.2 °C by the “shake-flask” technique.^[32] Substrate concentration in either phase was determined spectrophotometrically at the λ_{\max} of aggregated **FD1–5** (260 nm) in water and at the λ_{\max} of monomeric **FD1–5** (254 nm) in *n*-octanol. **FD1–5** solutions were centrifuged for 15 min at 3000 runs/min before the experiments and shaken for 24 h with a tube-rotator apparatus at 33 runs/min. The water/*n*-octanol volume ratio was 5:1 for **FD1–5**. The initial concentrations of the aqueous solutions of **FD1–5** were 5 \times 10⁻⁶ M.

UV/Visible Determinations: UV/Vis determinations were carried out on a Cary 1E Varian or a V550 Jasco spectrophotometer.

Transmission Electron Microscopy: Drops of a dilute solution of **FD3** (5 \times 10⁻⁵ M) were placed onto copper grids pre-coated with carbon and then evaporated at room temperature. The experiments were carried out on a FP 505 Morgagni Series 268D electron microscope (Philips) operating at 60 kV, equipped with a Megaview III digital camera and a Soft Imaging System (Germany).

Molecular Mechanics Calculations: The superficial area of the **FD1–5** molecules was calculated with the Hyperchem 6.03 program on an optimized conformation obtained with the MMFF Force Field as implemented in the Titan 1.0.1 package.^[33]

Synthesis of FD1–FD5: The synthetic details and appropriate literature citations for the preparation and characterization of fulleropyrrolidines **FD1–FD5** are available as Supporting Information (see footnote on the first page of this article).

Acknowledgements

We thank MIUR for financial support (COFIN 2002: protocol number 2002032171) and the CESI center of the University “G. d’Annunzio” for making the transmission electron microscope available. M.M. wish to thank the University of Padova (grant CPDA012428).

- [1] R. Taylor, D. R. M. Walton, *Nature* **1993**, 363, 685–693.
- [2] C. Brabec, N. Sariciftci, J. Hummelen, *Adv. Funct. Mater.* **2001**, 11, 15–16.
- [3] H. S. Nalwa, *Adv. Mater.* **1993**, 5, 341–358.
- [4] T. Da Ros, M. Prato, *Chem. Commun.* **1999**, 663–669.
- [5] H. Tokuyama, S. Yamago, E. Nakamura, T. Shiraki, Y. Sugiura, *J. Am. Chem. Soc.* **1993**, 115, 7918–7919.
- [6] R. Sijbesma, G. Srdanov, F. Wudl, J. A. Castoro, C. Wilkins, S. H. Fridman, D. L. De Camp, G. L. Kenyon, *J. Am. Chem. Soc.* **1993**, 115, 6510–6512.
- [7] D. I. Schuster, S. R. Wilson, R. F. Schinazi, *Bioorg. Med. Chem. Lett.* **1996**, 6, 1253–1256.
- [8] E. Nakamura, H. Isobe, *Acc. Chem. Res.* **2003**, 36, 807–815.
- [9] L. Y. Chiang, J. B. Bhonsle, L. Wang, S. F. Shu, T. M. Chang, J. Ru Hwu, *Tetrahedron* **1996**, 52, 4963–4972.
- [10] D. M. Guldi, H. Hungerbuhler, K. D. Asmus, *J. Phys. Chem.* **1995**, 99, 13487–13493.
- [11] D. M. Guldi, *J. Phys. Chem. A* **1997**, 101, 3895–3900.
- [12] G. Angelini, P. De Maria, A. Fontana, M. Pierini, M. Maggini, F. Gasparrini, G. Zappia, *Langmuir* **2001**, 17, 6404–6407.
- [13] N. Nakashima, T. Ishii, M. Shirakusa, T. Nakanishi, M. Murakami, T. Sagaralal, *Chem. Eur. J.* **2001**, 7, 1766–1772.
- [14] M. Sano, K. Oishi, T. Ishii, S. Shinkai, *Langmuir* **2000**, 16, 3773–3776.
- [15] C. F. Richardson, D. I. Schuster, S. R. Wilson, *Org. Lett.* **2000**, 2, 1011–1014.
- [16] All spectroscopic and analytical data of **FD2–5** were consistent with the proposed molecular structure (see Supporting Information)

- [17] V. Georgakilas, F. Pellarini, M. Prato, D. M. Guldi, M. Melle-Francot, F. Zerbetto, *Proc. Nat. Acad. Sci. USA* **2002**, *99*, 5075–5080.
- [18] A. M. Cassell, C. L. Asplund, J. M. Tour, *Angew. Chem. Int. Ed.* **1999**, *38*, 2403–2405.
- [19] T. Da Ros, M. Prato, F. Novello, M. Maggini, E. Banfi, *J. Org. Chem.* **1996**, *61*, 9070–9072.
- [20] G. V. Andrievsky, V. K. Klochkov, E. L. Karyakina, N. O. Mchedlov-Petrosyan, *Chem. Phys. Lett.* **1999**, *300*, 392–396.
- [21] The difference in absorbance was calculated from the following equation: $(\Delta\text{ABS}_{254430})_{\text{norm}} = (\Delta\text{ABS}_{\text{THF}_{\text{int}}} - \Delta\text{ABS}_{\text{THF}_{\text{min}}}) / (\Delta\text{ABS}_{\text{THF}_{\text{pure}}} - \Delta\text{ABS}_{\text{THF}_{\text{min}}}) \times 100$ where the subscripts THF_{min} , THF_{pure} and THF_{int} refer to differences in absorbance between 254 nm and 430 nm of FDs in the investigated solvent mixtures at minimum, maximum and intermediate percentages of THF, respectively.
- [22] L. R. Snyder, *Techniques of Chemistry* (Eds.: E. S. Perry, A. Weissberger), Plenum Press, New York, **1978**, chapter 2.
- [23] H. S. Frank, M. W. Evans, *J. Chem. Phys.* **1945**, *13*, 507.
- [24] F. Franks, in *Water, A Comprehensive Treatise, Vol. 4* (Ed.: F. Franks), Plenum Press, New York, **1973**, chapter 1.
- [25] P. L. Privalov, S. J. Gill, *Adv. Protein Chem.* **1988**, *39*, 191–234.
- [26] A. Nicholls, K. A. Sharp, H. Honig, *Proteins* **1991**, *11*, 281–296.
- [27] A. Vailaya, C. Horvath, *J. Phys. Chem. B* **1997**, *101*, 5875–5888.
- [28] O. Sinanoglu, *J. Chem. Phys.* **1981**, *75*, 463–468.
- [29] The κ value of any aqueous THF solution was calculated as a contribution's sum of κ values for H_2O and THF pure solvents, weighted on their molar fractions in the mixture. THF's κ value ($\kappa = 1.002$) was interpolated from the equation $\kappa = 0.0348\varepsilon + 0.7371$ ($r^2 = 0.993$) obtained from a κ vs. ε plot for the following solvents:^[28] ethanol, methanol, *n*-butanol, toluene, benzene, carbon tetrachloride, carbon disulfide and cyclohexane.
- [30] A. Vailaya, C. Horvath, *J. Phys. Chem. B* **1998**, *102*, 701–718.
- [31] a) W.-H. Shiu, K.-C. Ma, *J. Phys. Chem. Ref. Data* **2000**, *29*, 41–130; b) M. M. C. Ferreira, *Chemosphere* **2001**, *44*, 125–146.
- [32] J. C. Dearden, G. M. Bresnen, *Quant. Struct.-Act. Relat.* **1988**, *7*, 133–144.
- [33] Wavefunction, Inc., 18401 Von Karman Avenue, Suite 370, Irvine, CA 92612, USA.

Received: October 05, 2004